

Noncovalently Connected Frameworks with Nanoscale Channels Assembled from a Tethered Polyoxometalate–Pyrene Hybrid**

Yu-Fei Song, De-Liang Long, and Leroy Cronin*

Polyoxometalate (POM) clusters are of interest since their assembly can bridge multiple length scales^[1] from the assembly of sub-nanoscale to protein-sized molecules^[2] and even colloidal aggregates of clusters many hundreds of nanometers in size.^[3] Therefore the ability to bridge such length scales, coupled with their attractive electronic^[4] and molecular properties^[5] that give rise to a variety of applications in diverse fields, such as catalysis,^[6] medicine,^[7] or materials science offers interesting and exciting perspectives for the design of new materials,^[4–7] especially framework materials.^[8] Perhaps one of the most interesting aspects of POM chemistry lies with the fact that the clusters can be viewed as transferable building blocks. As such, the controlled assembly of polyoxometalate-based building blocks defines a crucial challenge to engineer the POM building blocks so they can assemble into novel architectures with functionality.^[1–8] An important extension to this building-block concept is realized by the use of POMs to form organic–inorganic hybrid compounds which comprise covalently connected cluster and organo fragments, thereby allowing the intermit combination of the properties of the metal–oxo and organic building blocks; this has been used to prepare polymers,^[9] dendrimers,^[10] and macroporous materials.^[11] It is apparent now that organic components can dramatically influence the microstructures of inorganic oxides, thus providing a way for the design of novel materials, and this has been shown in the natural world.^[12] In this respect, we are interested in the combination of highly conjugated organic molecules with POMs since this class of materials has hardly been explored, and should allow the assembly of interesting systems.^[13–15] Such organic–inorganic hybrid materials will not only combine the advantages of organic molecules, such as structural fine tuning, but also the close interaction and synergistic effects of organic group and inorganic cluster. However, the major limitation is that the covalent functionalization of POMs in general is not straightforward, depending critically upon the building blocks chosen. One route to achieve this goal is to use a flexible synthetic strategy, in which

the organic linker between the POMs and the organic site is designed to be bifunctional.^[16] Therefore we utilized Tris (tris(hydroxymethyl)aminomethane, (HOCH₂)₃NH₂), in combination with a manganese-Anderson-type (Mn-Anderson) POM^[17] and this was inspired by the work of Hasenknopf, Gouzerh et al., who first demonstrated the utility of this approach to construct potential hybrid POM–organic units.^[16–18]

Herein, we demonstrate the tethering of highly conjugated and planar pyrene units, derivatized with Tris yields [(HOCH₂)₃CNH-CH₂-C₁₆H₉] (**1**) and that the reaction of **1** with [N(C₄H₉)₄]₄[α-Mo₈O₂₆] and Mn(OAc)₃ in CH₃CN yields a novel building block that comprises a Mn-Anderson cluster tethered to two pyrene units through the Tris linker to give [Mn-Anderson(Tris-pyrene)₂]³⁻, that is, [MnMo₆O₁₈-(OCH₂)₃CNH-CH₂-C₁₆H₉]₂³⁻ (**2a**; Scheme 1; compound **2** is **2a** + counterions).

By tethering the highly delocalized aromatic pyrene moiety covalently to the Mn-Anderson-type cluster through the Tris connector, we have been able to modify the physical properties of the Mn-Anderson cluster dramatically,^[13] and this is shown in the UV/Vis absorption spectrum (Figure 1) and also in the fluorescence emission spectrum (see the Supporting Information).

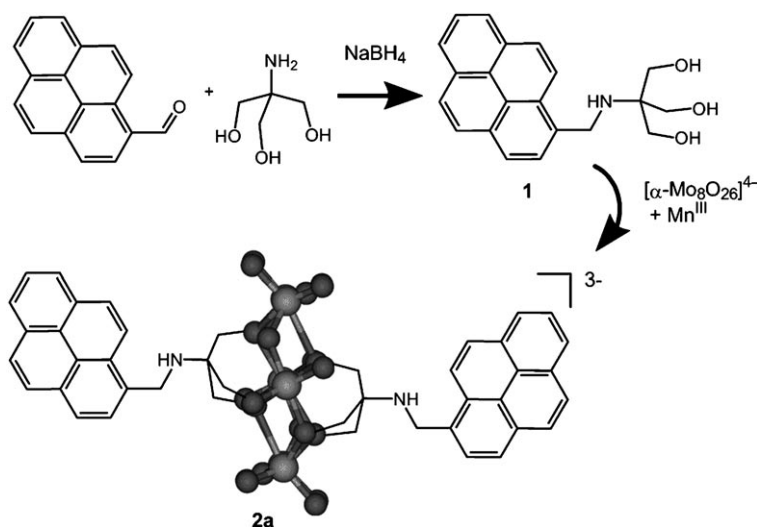
In comparison to the UV/Vis spectrum of the Mn-Anderson cluster itself, which only shows absorption at 217 nm and a shoulder peak at 245 nm, the absorption spectrum of **2** is dominated by pyrene vibronic progression.^[19] The steady-state fluorescence emission spectrum of the compound **2** shows one sharp peak at 380 nm with another very broad peak (see the Supporting Information) to lower energy at 413 nm (by ca. 2000 cm⁻¹). This peak is assigned to emission from the lowest excited single state of the pyrene chromophore and it shows that **2** is highly fluorescent compared to the underivatized Mn-Anderson cluster.^[19]

In addition, we show that the assembly in the presence of tetrabutylammonium (TBA) cations facilitates the construction of an unprecedented framework material [N(C₄H₉)₄]₃[MnMo₆O₁₈[(OCH₂)₃CNH-CH₂-C₁₆H₉]₂·2DMF·3H₂O] (**2**) with nanoscale channels that can reversibly bind aromatic guest molecules. This situation is remarkable since only very weak supramolecular interactions between the anionic building blocks, **2a** (this building block itself is built from a combination of coordinative and covalent interactions), and TBA, such as van der Waals and C–H···O=Mo hydrogen bonds are responsible for the structural integrity of the overall framework which is stable up to 240°C. The framework material **2** was isolated in 19% yield as very long needle crystals after diethyl ether diffusion into a DMF solution of the compound for one week. The crystals were characterized

[*] Dr. Y.-F. Song, Dr. D.-L. Long, Prof. L. Cronin
WestCHEM
Department of Chemistry
The University of Glasgow
Glasgow, G12 8QQ (UK)
Fax: (+44) 141-330-4888
E-mail: l.cronin@chem.gla.ac.uk

[**] This work was supported by the EPSRC and The University of Glasgow.

Supporting information for this article is available on the WWW under <http://www.angewandte.org> or from the author.



Scheme 1. Synthetic route to the formation of the $[\text{Mn-Anderson}(\text{Tris-pyrene})_2]^{3-}$ building block $[\text{MnMo}_6\text{O}_{18}\{(\text{OCH}_2)_3\text{CNH-CH}_2\text{-C}_{16}\text{H}_9\}_2]^{3-}$ (**2a**). The oxygen atoms of the Anderson cluster are shown as smaller darker spheres, the metal atoms as larger lighter spheres.

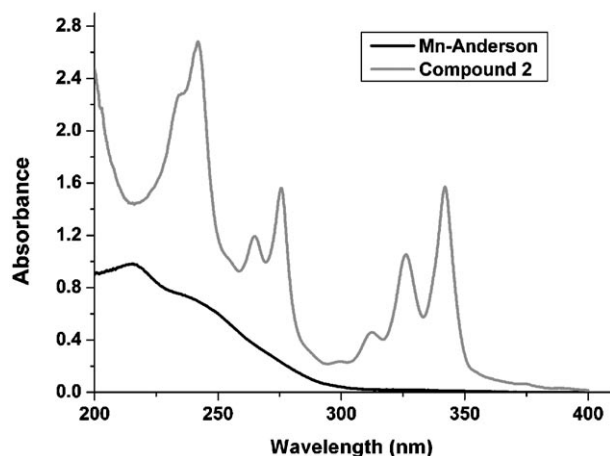


Figure 1. a) UV/Vis spectra of the underivatized Mn-Anderson cluster and **2**. For **2**: λ (ϵ) = 242 (1.8×10^5), 264 (8.1×10^4), 275 (9.3×10^4), 312 (3.0×10^4), 326 (6.9×10^4), 341 (9.1×10^4), 375 nm ($3600 \text{ L cm}^{-1} \text{ mol}^{-1}$); all spectra were run at room temperature.

by single-crystal X-ray structure analyses,^[20] NMR, UV/Vis, IR, and fluorescence emission spectroscopy, electrochemistry, differential scanning calorimetry (DSC), thermogravimetric analysis (TGA), ESI-MS, and elemental analyses, as well as solid-state guest-uptake measurements.

X-ray crystallographic analysis of **2** shows that the asymmetric unit consists of 1.5 $[\text{Mn-Anderson}(\text{Tris-pyrene})_2]^{3-}$ ions (one Mn-Anderson cluster is located in a normal position, while the other half Mn-Anderson cluster is located at an inversion center), along with 4.5 TBA cations (the 0.5 TBA cation is ill-defined and disordered over an inversion centre). 3 DMF and 4.5 H_2O solvent molecules were located crystallographically and give a slightly larger solvent content than found using elemental analysis and TGA. The overall unit cell contains 12 Anderson-cluster units with

24 pyrene units, and 36 TBA cations which surround nanoscale 1D channels that run parallel to the crystallographic *b* axis. These channels are butterfly shaped and are approximately 1 nm wide and 2 nm long and are filled with DMF and water molecules. Indeed, the solvent-accessible void present in these channels is large, measuring approximately 10000 \AA^3 , some 30% of the total unit-cell volume (Figure 2).

The main structure-directing building block present in **2** is the Mn-Anderson cluster, which comprises six edge-sharing $\{\text{MoO}_6\}$ octahedra arranged around a central $\{\text{MnO}_6\}$ unit. The alkoxy “arms” of the Tris ligand are bound to the Mn^{III} ion and the rigidity of the pocket defined by the six edge-sharing $\{\text{MoO}_6\}$ octahedra, prevents the Mn^{III} ion from displaying a marked Jahn–Teller distortion. The two Tris moieties cap both sides of hexagon and the cluster framework is linked through a C–N single bond to the organic pyrene groups. The formation of the framework is facili-

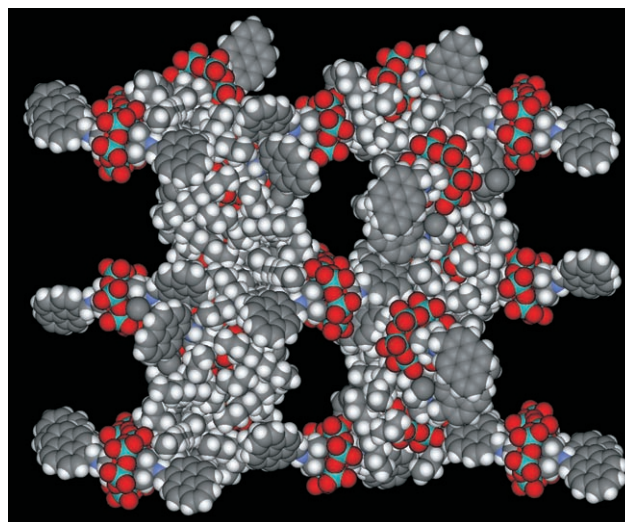


Figure 2. Space-filling representation of the framework in **2** projected onto the crystallographic *ac* plane. The butterfly-shaped 1D channels are clearly seen. The walls of the channels comprise the Mn-Anderson cluster core, pyrene, and TBA moieties. Mo green, C black, H white, N blue, O red (Mn hidden in this view).

tated by the two types of $[\text{Mn-Anderson}(\text{Tris-pyrene})_2]^{3-}$ building blocks present in the structure (labeled **A** and **B** in Figure 3), and they connect the structure in totally different ways. Type **A** $[\text{Mn-Anderson}(\text{Tris-pyrene})_2]^{3-}$ building blocks have each of the two C–N bond vectors connecting to the pyrene units arranged *syn* to each other and the planes running through the aromatic units are positioned at approximately 170° to each other whereas in type **B** the C–N bond vectors are arranged *anti* to each other and the planes running through the aromatic units are almost co-planar.

The cluster unit present in type **A** building blocks acts as an acceptor unit for C–H hydrogen bond-like interactions

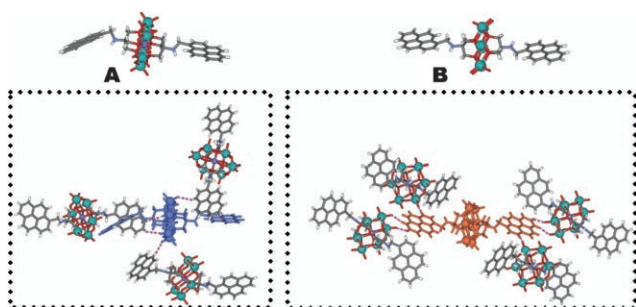


Figure 3. The two types of $[\text{Mn-Anderson}(\text{Tris-pyrene})_2]^{3-}$ building blocks, **A** and **B** (top), and sections of the structure (bottom) containing the building blocks **A** (blue) and **B** (orange). The weak $\text{C-H}\cdots\text{O}=\text{Mo}$ interactions are shown by the purple dotted lines: the type **A** building blocks act as acceptors, and type **B** building blocks as donors. Mo green, Mn purple, C black, H white, N blue, O red.

from the pyrene units of type **B** building blocks ($\text{C-H}\cdots\text{O}=\text{Mo}$ range 2.4–2.7 Å) and the pyrene units of type **A** building blocks can also act as donors to provide C-H units to interact with the cluster core of other type **A** building blocks. The type **B** building blocks act as C-H donors, in this case the cluster unit is passive and only interacts very weakly with TBA counteranions. Therefore only the geometry of the linkage between the cluster ligated with Tris and the two pyrene units is able to define the donor–acceptor characteristics of the building blocks. Indeed the 1D channels present are constructed by a ring of building blocks arranged in a (-A-B-A-A-B-A-) configuration and stacks of these rings form the channels (Figure 4).

Investigation of the stability of **2** was initially carried out using TGA which showed that the DMF and water molecules are lost below 180°C (ca. 9% of the total weight) and this is followed by a plateau around 240–250°C and then a weight loss corresponding to the decomposition and loss of three TBA cations per $\text{Anderson}(\text{Tris-pyrene})_2$ unit (Figure 5).

DSC measurements show a very sharp endothermic feature at 237°C followed by series of two exothermic features at 238 and 240°C, respectively. Visually the compound melts at around 237–240°C so we suggest that the

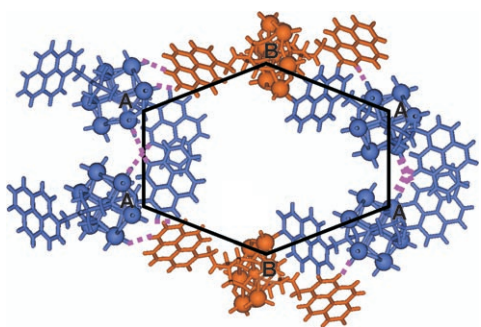


Figure 4. The walls of the pores are formed by $[\text{Mn-Anderson}(\text{Tris-pyrene})_2]^{3-}$ building blocks (**A** blue, **B** orange) so that they are held together in a (-A-B-A-A-B-A-) fashion by weak $\text{C-H}\cdots\text{O}=\text{Mo}$ interactions (purple dotted lines) in the crystallographic ac plane. Stacks of these building blocks form the channel, which runs down the crystallographic b axis.

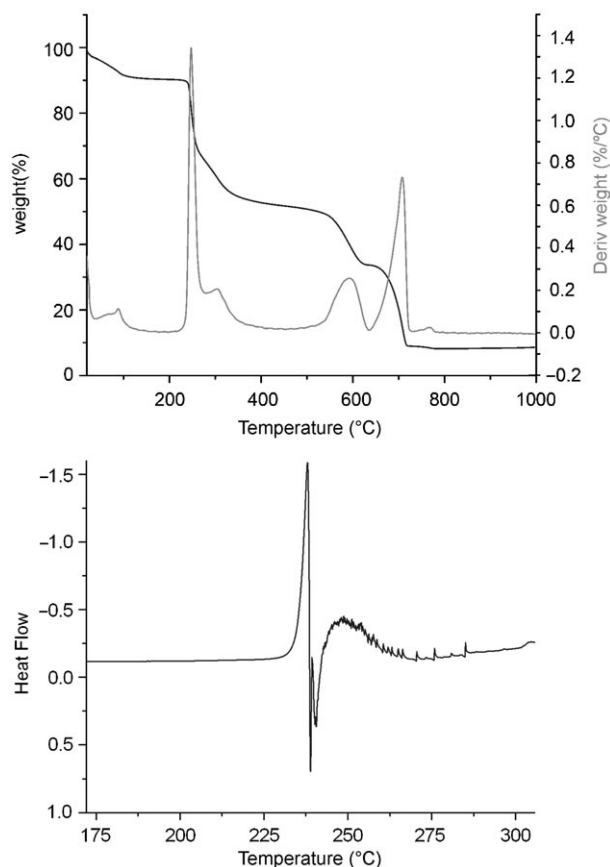


Figure 5. TGA (top) and DSC (bottom) curves of **2**. The TGA curve shows (weight loss = black line; derivative of weight loss = gray line) loss of solvent between room temperature and 200°C. At 250°C TBA loss is observed before decomposition of the cluster unit. The DSC curve shows a very rapid melting and recrystallization process at 240°C that occurs over only a few degrees before TBA loss.

“melting” process seen in the DSC can be assigned to the collapse of the porous structure and formation of a denser phase just before the decomposition and loss of the TBA counter ions. Therefore these studies indicate that the structural integrity of this framework material to be intact to approximately 240°C, which appears remarkable for such a class of material connected together using very weak interactions.

To see if the material is able to uptake other guests, exploiting the porosity that appears to be structurally present, vapor absorption experiments were undertaken with chlorobenzene and the contents of the framework were evaluated using ^1H NMR spectroscopy. These studies show (see the Supporting Information) clearly that the framework can absorb a large quantity of chlorobenzene corresponding to three chlorobenzene units per cluster (this corresponds to an uptake of 12% by mass). Furthermore, the loss of the porosity associated with framework collapse is confirmed by experiments with chlorobenzene performed on material heated above 240°C; these experiments show no guest uptake. In addition, preliminary UV/Vis measurements indicate that compound **2** is potentially many times more selective for chlorobenzene uptake than for cyclohexane.

In conclusion, we have grafted of a highly delocalized aromatic ring system based on pyrene to a Mn-Anderson cluster to produce an organic-inorganic hybrid building block with physical properties that are fundamentally different to the parent polyoxometalate cluster. Furthermore the self assembly of this [Mn-Anderson(Tris-pyrene)₂]³⁻ building block with TBA cations produces a nanoporous framework with nanoscale solvent-accessible 1D channels. This material appears to be stable until 240 °C despite being constructed from very weak CH...O=Mo hydrogen bonding interactions. Further, the network is built from two types of [Mn-Anderson(Tris-pyrene)₂]³⁻ ions that differ only in the relative orientations of the pyrene "arms" that are anchored to the Mn-Anderson-type cluster, yet appear to totally alter the donor-acceptor characteristics of the building blocks. The type **A** [Mn-Anderson(Tris-pyrene)₂]³⁻ building block, in which the arms are slightly compressed, mainly accepts C-H hydrogen bonds from the other pyrene moieties, whereas the type **B** building blocks, in which the arms are fully extended and coplanar, exclusively donates C-H hydrogen bonds. Finally, guest-uptake measurements have shown that the framework is nanoporous and it is able to absorb up to 12% by weight of chlorobenzene. In further work, we will examine the competitive guest absorption and attempt to extend the building-block principle reported herein in the construction of other frameworks, and to utilize the new physical properties of the building blocks for application as catalysts, sensors, and new optically interesting materials.

Experimental Section

1: Compound **1** was synthesized typically by reaction of (HOCH₂)₃CNH₂ (Tris, 2.0 g, 16.5 mmol) with 1-pyrenecarbaldehyde (3.8 g, 16.5 mmol) in MeOH (100 mL) and the resulting Schiff base was reduced by NaBH₄ (0.91 g, 24.8 mmol). The reaction mixture was evaporated to dryness under vacuum and dissolved in water (100 mL). After the addition of HCl (4 M, 30 mL), the water solution was extracted with CH₂Cl₂ (300 mL). NaOH solution (4 M, 100 mL) was added to the aqueous phase, and the resulting solution was evaporated to dryness. Dry ethanol (50 mL) was added, and the reaction mixture was then stirred for 10 min at 0 °C. A light-yellowish solid was isolated by filtration and dried under vacuum. Yield: 67% (3.7 g). Elemental analysis (%) calcd for C₂₁H₂₁O₃N (335 g mol⁻¹): C 75.2, H 6.3, N 4.2; found C 75.5, H 6.8, N 4.0. ESI-MS ([MH]⁺): 336 g mol⁻¹. IR (KBr): $\tilde{\nu}$ = 2926 (m), 2878 (m), 2853 (m), 1670 (m), 1458 (s), 1354 (m), 1244 (w), 1188 (m), 1117 (s), 1042 (s), 937 (s), 843 (s), 717 (m), 549 (m), 497 cm⁻¹ (m). ¹H NMR (400 MHz; [D₄]MeOD): δ = 3.73 (s, 2H, -CH₂-), 3.88 (br, 6H, -CH₂-), 8.01 (t, *J* = 8 Hz, 1H, -CH-), 8.10 (s, 2H, -CH-), 8.22 (m, 5H, -CH-), and 8.57 ppm (d, *J* = 10 Hz, 1H, -CH-).

2: A mixture of [N(C₄H₉)₄][α -Mo₃O₂₆] (8.0 g, 3.7 mmol), MnOAc₃·2H₂O (1.5 g, 5.6 mmol) and compound **1** (4.29 g, 12.8 mmol) were kept refluxing in MeCN for 24 h, and the resulting brown precipitate was removed by filtration. The filtrate was evaporated to dryness under vacuum, and the resulting solid was dissolved in a small amount of DMF. Diffusion of diethyl ether into the DMF solution resulted, over one week, in the formation of long needle crystals suitable for X-ray crystallography. Yield: 19% (2.3 g, based on Mo). Melting point: 239–240 °C. Elemental analysis (%) calcd for C₉₆H₁₆₄MnMo₆N₇O₂₉ (2510.9 g mol⁻¹): C 45.9, H 6.6, N 3.9; found C 45.7, H 6.8, N 4.0. ESI-MS (negative mode): 2067 g mol⁻¹ ([M-2DMF-3H₂O-TBA]⁻). IR (KBr): $\tilde{\nu}$ = 2957 (m), 2933 (m), 2868 (m), 1668 (s), 1479 (s), 1383 (m), 1249 (w), 1071 (m), 1032 (m), 938 (s), 918 (s), 851 (w), 664 cm⁻¹ (s).

¹H NMR (400 MHz; [D₆]DMSO): 0.94 (t, *J* = 8.0 Hz, 36H, 4-H_{TBA}), 1.25 (m, 24H, 3-H_{TBA}), 1.57 (m, 24H, 2-H_{TBA}), 2.73 (s, 6H, -CH₃ (2DMF)), 2.90 (s, 6H, -CH₃ (2DMF)), 3.15 (m, 24H, 1-H_{TBA}), 4.0 (broad, 4H, -CH₂-), 7.92 (s, 2H, -CH-), 8.08 (t, *J* = 8.0 Hz, 2H, -CH-), 8.17 (m, 4H, -CH-), 8.28 (d, *J* = 8.0 Hz, 8H, -CH-), 8.35 (broad, 2H, -CH-), 62.5 ppm (broad, 12H, CH₂O).

Received: November 21, 2006

Published online: April 11, 2007

Keywords: Organic-inorganic hybrid compounds · polyoxometalates · porous materials · pyrene · supramolecular interactions

- [1] D. L. Long, L. Cronin, *Chem. Eur. J.* **2006**, *12*, 3698.
- [2] A. Müller, E. Beckmann, H. Bögge, M. Schmidtman, A. Dress, *Angew. Chem.* **2002**, *114*, 1210; *Angew. Chem. Int. Ed.* **2002**, *41*, 1162.
- [3] T. B. Liu, E. Diemann, H. L. Li, A. W. M. Dress, A. Müller, *Nature* **2003**, *426*, 59.
- [4] D. L. Long, H. Abbas, P. Kögerler, L. Cronin, *Angew. Chem.* **2005**, *117*, 3387; *Angew. Chem. Int. Ed.* **2005**, *44*, 3415; M. T. Pope, *Prog. Inorg. Chem.* **1991**, *39*, 181.
- [5] A. Müller, S. Roy, *Coord. Chem. Rev.* **2003**, *245*, 153.
- [6] W. B. Kim, T. Voitl, G. J. Rodriguez-Rivera, S. T. Evans, J. A. Dumesic, *Angew. Chem.* **2005**, *117*, 788; *Angew. Chem. Int. Ed.* **2005**, *44*, 778; W. B. Kim, T. Voitl, G. J. Rodriguez-Rivera, J. A. Dumesic, *Science* **2004**, *305*, 1280; B. Botar, Y. V. Geletii, P. Kogerler, D. G. Musaev, K. Morokuma, I. A. Weinstock, C. L. Hill, *J. Am. Chem. Soc.* **2006**, *128*, 11268.
- [7] D. A. Judd, J. H. Nettles, N. Nevins, J. P. Snyder, D. C. Liotta, J. Tang, J. Ermolieff, R. F. Schinazi, C. L. Hill, *J. Am. Chem. Soc.* **2001**, *123*, 886.
- [8] A. Dolbecq, C. Mellot-Draznieks, P. Mialane, J. Marrot, G. Férey, F. Sécheresse, *Eur. J. Inorg. Chem.* **2005**, 3009; S. Kitagawa, R. Kitaura, S. Noro, *Angew. Chem.* **2004**, *116*, 2388; *Angew. Chem. Int. Ed.* **2004**, *43*, 2334; J. L. C. Rowsell, O. M. Yaghi, *Angew. Chem.* **2005**, *117*, 4723; *Angew. Chem. Int. Ed.* **2005**, *44*, 4670; G. Férey, C. Mellot-Draznieks, C. Serre, F. Millange, J. Dutour, S. Surléy, I. Margiolaki, *Science* **2005**, *309*, 2040.
- [9] B. B. Xu, M. Lu, J. H. Kang, D. G. Wang, J. Brown, Z. H. Peng, *Chem. Mater.* **2005**, *17*, 2841; A. R. Moore, H. Kwen, A. M. Beatty, E. A. Maatta, *Chem. Commun.* **2000**, 1793.
- [10] H. D. Zeng, G. R. Newkome, C. L. Hill, *Angew. Chem.* **2000**, *112*, 1841; *Angew. Chem. Int. Ed.* **2000**, *39*, 1772.
- [11] R. C. Schroden, C. F. Blanford, B. J. Melde, B. J. S. Johnson, A. Stein, *Chem. Mater.* **2001**, *13*, 1074.
- [12] P. J. Hagrman, D. Hagrman, J. Zubieta, *Angew. Chem.* **1999**, *111*, 2798; *Angew. Chem. Int. Ed.* **1999**, *38*, 2639.
- [13] B. B. Xu, Y. G. Wei, C. L. Barnes, Z. H. Peng, *Angew. Chem.* **2001**, *113*, 2353; *Angew. Chem. Int. Ed.* **2001**, *40*, 2290; Z. H. Peng, *Angew. Chem.* **2004**, *116*, 948; *Angew. Chem. Int. Ed.* **2004**, *43*, 930.
- [14] J. L. Stark, A. L. Rheingold, E. A. Maatta, *J. Chem. Soc. Chem. Commun.* **1995**, 1165; J. B. Strong, G. P. A. Yap, R. Ostrander, L. M. Liable-Sands, A. L. Rheingold, R. Thouvenot, P. Gouzerh, E. A. Maatta, *J. Am. Chem. Soc.* **2000**, *122*, 639.
- [15] J. L. Stark, V. G. Young, E. A. Maatta, *Angew. Chem.* **1995**, *107*, 2751; *Angew. Chem. Int. Ed. Engl.* **1995**, *34*, 2547. H. Kwen, V. G. Young, E. A. Maatta, *Angew. Chem.* **1999**, *111*, 1215; *Angew. Chem. Int. Ed.* **1999**, *38*, 1145.
- [16] P. R. Marcoux, B. Hasenknopf, J. Vaissermann, P. Gouzerh, *Eur. J. Inorg. Chem.* **2003**, 2406.

- [17] B. Hasenknopf, R. Delmont, P. Herson, P. Gouzerh, *Eur. J. Inorg. Chem.* **2002**, 1081.
- [18] S. Favette, B. Hasenknopf, J. Vaissermann, P. Gouzerh, C. Roux, *Chem. Commun.* **2003**, 2664.
- [19] B. Bodenant, F. Fages, M. H. Delville, *J. Am. Chem. Soc.* **1998**, *120*, 7511.
- [20] Crystal data and structure refinements for compound **2**: $C_{96}H_{164}MnMo_6N_7O_{29}$, $M_r = 2510.9 \text{ g mol}^{-1}$. A brown needle crystal ($0.20 \times 0.20 \times 0.10 \text{ mm}^3$) was measured on a Bruker Apex II CCD diffractometer using MoK_{α} radiation ($\lambda = 0.71073 \text{ \AA}$) at 100(2) K. Orthorhombic, space group $Pbca$, $a = 43.9365(12)$, $b = 15.7008(5)$, $c = 54.326(2) \text{ \AA}$, $V = 37476(2) \text{ \AA}^3$, $Z = 12$, $\rho = 1.335 \text{ g cm}^{-3}$, $F(000) = 15576$. 88953 reflections measured ($2\theta_{\text{max}} = 40.9^\circ$), 18139 unique ($R_{\text{int}} = 0.1236$), 10766 observed ($I > 2\sigma(I)$). $R1 = 0.0858$, $wR2$ (all data) = 0.2626. CCDC-627617 contains the supplementary crystallographic data for this paper. These data can be obtained free of charge from The Cambridge Crystallographic Data Centre via www.ccdc.cam.ac.uk/data_request/cif.
-